Geophys. J. R. astr. Soc. (1978) **52**, 503–524

Transient and impulse responses of a one-dimensional linearly attenuating medium – II. A parametric study

J. B. Minster *Seismological Laboratory, Division of Geological and Planetary Sciences, California Institute of Technology, Pasadena, California 91125, USA*

Received 1977 August 19; in original form 1977 May 18

Summary. We investigate one-dimensional waves in a standard linear solid for geophysically relevant ranges of the parameters. The critical parameters are shown to be $T^* = t_u/Q_m$ where t_u is the travel time and Q_m the quality factor in the absorption band, and τ_m^{-1}, the high-frequency cut-off of the relaxation spectrum. The visual onset time, rise time, peak time, and peak amplitude are studied as functions of T^* and τ_m. For very small τ_m, this model is shown to be very similar to previously proposed attenuation models. As τ_m grows past a critical value which depends on T^*, the character of the attenuated pulse changes. Seismological implications of this model may be inferred by comparing body wave travel times with a 'one second' earth model derived from long-period observations and corrected for attenuation effects assuming a frequency independent Q over the seismic band. From such a comparison we speculate that there may be a gap in the relaxation spectrum of the Earth's mantle for relaxation times shorter than about one second. However, observational constraints from the attenuation of body waves suggest that such a gap might in fact occur at higher frequencies. Such a hypothesis would imply a frequency dependence of Q in the Earth's mantle for short-period body waves.

Introduction

In part I of this work, hereafter denoted Paper I, (Minster 1978), the evolution of transient (step-function) and impulsive (delta function) plane waves in a linearly attenuating medium was investigated analytically. The method involved a Laplace transform technique and the inverse transform was evaluated asymptotically for long propagation times by the method of steepest descent. The attenuation model consisted of a spectrum of independent relaxation mechanisms, the distribution function of which decreased hyperbolically with increasing relaxation characteristic time, within a given finite range. Following Anderson *et al.* (1977) we called this range the absorption band.

It was shown in Paper I that a suitable modification of the saddle point method yields an accurate first motion approximation to the transient and impulse responses as long as the

propagation time remains long with respect to the shortest relaxation time. Favourable comparison against previously published results indicated that the waveforms so obtained could be used for seismological applications.

The purpose of this paper resides in a systematic parametric investigation of the properties of such attenuated waveforms. After a brief recall of the general theoretical results we shall describe the results of a large number of calculations in which the parameters are varied within geophysically relevant ranges. Finally we shall discuss some of the most striking implications of this model for body wave seismology.

1 Summary of general results

The theory developed in Paper I pertains to a linear attenuation model based on the rheology of a standard linear solid (e.g. Liu, Anderson & Kanamori 1976; Anderson *et al.* 1977; Kanamori & Anderson 1977). The distribution function of the relaxation spectrum is assumed to be

$$D(\tau) = \frac{D}{\tau} H(\tau - \tau_m) H(\tau_M - \tau), \tag{1.1}$$

(e.g. Gurevich 1964). In that case the complex modulus is

$$\mathscr{R}(\omega) = M_u \left[1 + \frac{2}{\pi Q_m} \ln \frac{i\omega + \tau_M^{-1}}{i\omega + \tau_m^{-1}}\right], \tag{1.2}$$

where M_u is the 'unrelaxed' modulus of the medium. The 'relaxed' modulus is obtained by

$$M_R = \lim_{\omega \to 0} R(\omega) = M_u \left[1 - \frac{2}{\pi Q_m} \ln \frac{\tau_M}{\tau_m}\right]. \tag{1.3}$$

The quality factor is a function of frequency, and takes the minimum value Q_m for $\tau_M^{-1} \ll \omega \ll \tau_m^{-1}$. Expressions for the phase and group velocities, $Q(\omega)$, and the attenuation coefficient $\alpha(\omega)$ are given in (Paper I) as well as in the papers quoted above. We define V_u and V_R as the 'unrelaxed' and 'relaxed' wave speeds (phase velocities).

Fig. 1 depicts the various functions describing the absorption band for the following values of the parameters:

(a) $\tau_M = 10^{+4}$ s, $\tau_m = 10^{-2}$ s, $Q_m = 125$,

(b) $\tau_M = 10^{+2}$ s, $\tau_m = 10^{-2}$ s, $Q_m = 125$,

(c) $\tau_M = 10^{+2}$ s, $\tau_m = 10^{-4}$ s, $Q_m = 125$.

Fig. 1(a) shows the frequency dependence of $Q^{-1}(f)$. At the cost of a minor loss of symmetry we chose to use the frequency f instead of $\omega = 2\pi f$ for the horizontal axis. For small attenuation, we have to a good approximation (e.g. Paper I)

$$Q^{-1}(\omega) \simeq \frac{2}{\pi Q_m} \tan^{-1} \frac{\omega(\tau_M - \tau_m)}{1 + \omega^2 \tau_M \tau_m}. \tag{1.4}$$

The points at which $Q^{-1}(\omega)$ is half of its maximum value occur for $\omega = \tau_M^{-1}$ and τ_m^{-1} respectively. In terms of frequency, this means that the half amplitude points are attained for

$$f_m = \frac{1}{2\pi\tau_M}, \quad f_M = \frac{1}{2\pi\tau_m},$$

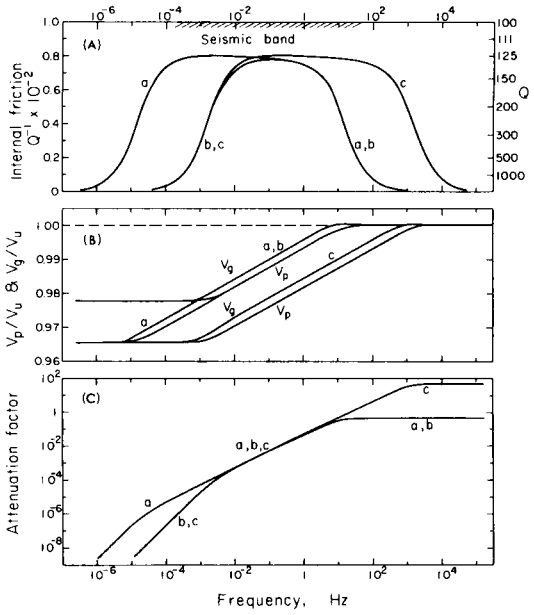

Figure 1. Quality factor, phase velocity and group velocity dispersion curves, and attenuation coefficient, as functions of frequency for several absorption bands. Parameters are given in the text.

respectively; in addition, Fig. 1(a) shows that $Q^{-1}(f)$ begins to decrease significantly for

$$f \lesssim 10 f_m, \quad f \gtrsim f_M/10.$$

Fig. 1(b) shows the dispersion curves associated with these various absorption bands. The phase velocity $V_p(f)$ and the group velocity $V_g(f)$ have been normalized to V_u. It is noteworthy that in a limited frequency band about f_M, $V_g(f) > V_u$, so that we observe an anomalous dispersion. Such phenomena are well known in electromagnetic theory (e.g. Brillouin 1960; Elices & García-Moliner 1968), and imply that the concept of group velocity loses its classical meaning in such frequency bands.

Fig. 1(c) represents the attenuation coefficient $\alpha(f)$. Its frequency dependence is proportional to f^2 at long periods, to f within the absorption band, and $\alpha(f)$ reaches a constant value at high frequencies.

In Paper I, we derived asymptotic approximations for the one-dimensional transient and impulse responses $u(t, x)$ and $v(t, x)$ respectively, of a medium with dissipation as described on Fig. 1. It was shown that:

(1) such approximations are uniformly good for travel time $t_u \gg \tau_M$;

(2) by suitable modifications of the method of steepest descent a good first motion approximation is obtained as long as $t_u \gg \tau_m$;

(3) the main – 'visible' – part of the signal is preceded by an exponentially small precursor. The character of this precursor was analysed in some detail;

(4) if V_s is the signal velocity, then $V_R < V_s < V_u$. V_s tends to V_u if t_u is rather small and Q_m rather large, or if τ_m is not too small. V_s tends to V_R as $t_u \to \infty$ (e.g. Chu 1962).

The purpose of this paper is to quantify these conclusions, for geophysically reasonable ranges of the parameters. The actual analytical expressions for the precursors, the transient

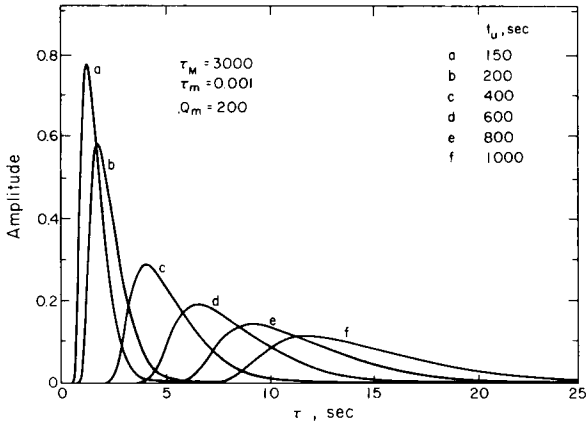

Figure 2. Degradation of an attenuated pulse with increasing travel time. Pulses are referred to the high frequency, unrelaxed arrival time in each case.

response signal and the impulse response signal are given in Paper I and will not be repeated here.

As a starting point for the discussion presented in the following section, the evolution of the impulse response as a function of increasing propagation time is depicted on Fig. 2. The parameters are

$$\tau_m = 0.001 \text{ s}, \quad \tau_M = 3000 \text{ s}, \quad Q_m = 200,$$

and the impulse response is shown for a wide range of propagation times listed on the figure.

The theoretical arrival time is defined by $t_u = x/V_u$, where x is the distance. In the remainder of the paper, waveforms will always be calculated from the expressions derived in Paper I, and will always be shown as functions of $\tau = t - t_u$. The outstanding features directly observable on Fig. 2 are:

(1) the peak amplitude steadily decreases, grossly as $1/t_u$;

(2) the peak time, the visual onset time, and the rise time (all defined on Fig. 3 below) all increase as t_u increases.

These features are in general agreement with the results published by various authors for a variety of linear attenuation models. We shall now study them in greater detail.

2 A parametric study of the attenuated waveforms

The parameters which characterize a particular attenuation model are τ_m, τ_M, Q_m, and t_u. Our approach will be to determine which combinations of these parameters control specific features of the attenuated waveforms.

The parameters we shall focus on in this section are described in Fig. 3. They comprise the peak amplitude A_p, the (reduced) peak time τ_p; the (reduced) visual onset time, hereafter called arrival time τ_a is defined by an *ad hoc* criterion: this is the time at which the amplitude reaches the value $A_p/1000$, that is, the amplitude is 60 db below the peak amplitude. This is the criterion used by Strick (1970). The rise time T_r is defined by the criterion adopted by Stacey *et al.* (1975), which uses the steepest tangent to the waveform; the figure

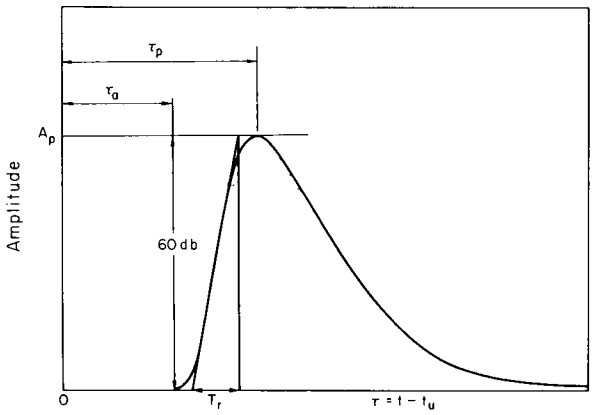

Figure 3. Parameters used in this study to characterize an attenuated pulse. τ_a is the 'arrival' time, τ_p the peak time, A_p the peak amplitude, T_r the rise time.

is self explanatory. We now turn to a systematic parametric investigation of the variation of these waveform parameters $(A_p, \tau_p, \tau_a, T_r)$ with the model parameters $(\tau_m, \tau_M, Q_m, t_u)$.

2.1 PROPAGATION TIME AND QUALITY FACTOR

Let us consider the transient (step-function) response $u(t, x)$. From the results of Paper I we know that its Fourier transform is of the form

$$\bar{u}(\omega, x) = \frac{\exp\left[\left[i\omega[t - x\sqrt{\rho}R^{-1/2}(\omega)]\right]\right]}{\omega}. \tag{2.1}$$

The exponent is therefore given by

$$\bar{F}(\omega) = i\omega t_u \left\{\frac{\tau}{t_u} + 1 - \left[1 + \frac{2}{\pi Q_m} \ln \frac{i\omega + \tau_M^{-1}}{i\omega + \tau_m^{-1}}\right]^{-1/2}\right\}. \tag{2.2}$$

For low-loss media, Q_m is large and

$$\bar{F}(\omega) \simeq i\omega\left[\tau + \frac{t_u}{\pi Q_m} \ln \frac{i\omega + \tau_M^{-1}}{i\omega + \tau_m^{-1}}\right]. \tag{2.3}$$

It is immediately clear that in the low-loss approximation the waveform as a whole depends only on the ratio $T^* = t_u/Q_m$. This result, which is a first-order approximation has been widely used in seismology (e.g. Anderson & Kovach 1964; Carpenter 1967; Helmberger & Wiggins 1971). For mantle body waves, suitable values of T^* are usually taken to be $T^* \simeq 1$ for P waves, and $T^* \simeq 4$ for S waves.

Fig. 4 shows several transient and impulse responses for the following values of the parameters:

$$\tau_m = 0.01 \text{ s}, \quad \tau_M = 5000 \text{ s}, \quad Q_m = 50, 100, 300, 1000.$$

In Fig. 4(a), t_u was chosen so that $T^* = 1$ in each case, and Fig. 4(b) corresponds to $T^* = 4$. It is clear that the waveforms are only weakly dependent on t_u (or Q_m) if T^* is held constant. The visual onset time, rise time, peak time, as well as the peak amplitude vary very

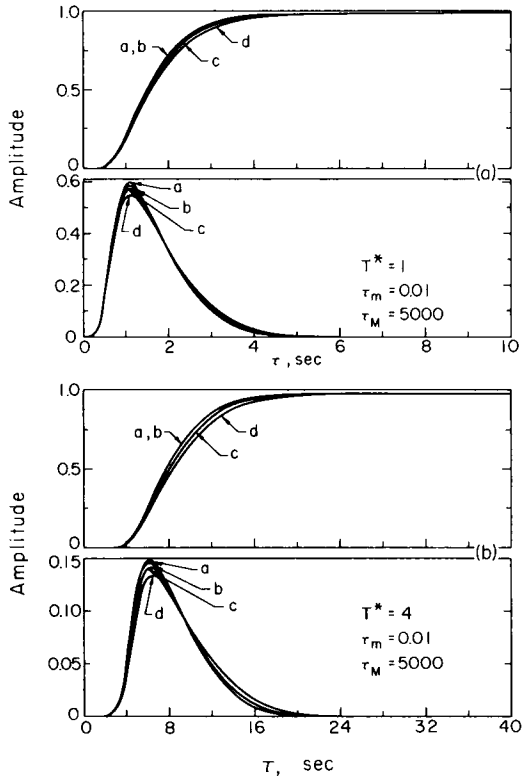

Figure 4. Transient responses and impulse responses for the two cases $T^* = 1$ and $T^* = 4$. The various curves correspond to (a) $Q_m = 1000$, (b) $Q_m = 300$, (c) $Q_m = 100$, (d) $Q_m = 50$.

little for the broad range of variation of Q_m. Only when Q_m becomes small – of the order of 50 – does the effect become more important. This is precisely the circumstance for which the approximation (2.3) begins to deteriorate.

Thus, for our present purpose, the list of parameters upon which the waveform may strongly depend is reduced to τ_m, τ_M, and T^*.

2.2 LONG-PERIOD CUT-OFF OF THE ABSORPTION BAND

It was argued in Paper I that the impulse response should be very insensitive to the long-period cut-off of the absorption band. This statement is illustrated on Fig. 5. The parameters were chosen as follows:

$$\tau_m = 0.01 \text{ s}, \quad t_u = 1000 \text{ s}, \quad Q_m = 250, \quad T^* = 4.$$

The three curves on Fig. 5 correspond to $\tau_M = 10^2$, 10^3 and 10^4 s respectively; it is clear that only the coda of the attenuated waveform is affected by τ_M. This is in agreement with the conclusion reached in Paper I. However, one must recall that the approximation developed in Paper I is essentially a first-motion approximation, which is not particularly accurate past the peak of the attenuated pulse. Thus the actual details of the fall-off of such pulses cannot be obtained with great precision from our calculations. Therefore the only conclusion we may safely reach from the analysis of Fig. 5 is that the effect of τ_M on the pulse shape is

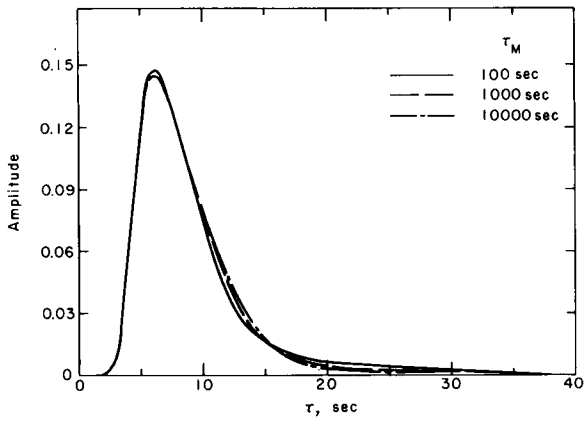

Figure 5. Effect of the long period cut-off τ_M of the absorption band on attenuated pulses. Parameters are described in the text.

rather subtle and that little can be learned about the long-period end of the absorption band from study of the impulse response. This agrees with what one might have predicted intuitively since the energy spectrum of a Dirac pulse in displacement falls off as ω^2 as $\omega \to 0$, so that the long-period components have little energy content. In order to gain information about the attenuation properties of the Earth at long periods, one may turn to the study of free oscillations (Anderson & Hart 1977; Hart 1977; Geller & Stein 1977). Thus the waveform parameters which we are interested in depend essentially on the two model parameters τ_m and T^*.

2.3 HIGH-FREQUENCY CUT-OFF OF THE ABSORPTION BAND

In order to evaluate the dependence of the pulse shape on τ_m and T^*, we chose $\tau_M = 1000$ s and $Q_m = 100$, and let τ_m vary from 0.1 to 10^{-5} s for the two values $T^* = 1$ and $T^* = 4$. The corresponding pulses are shown on Fig. 6(a) and (b) respectively.

It is clear that τ_m and T^* have a drastic effect on the attenuated pulse. At fixed T^*, and for increasing τ_m, both parameters τ_a and τ_p increase steadily. On the other hand, the peak amplitude A_p and the rise time T_r appear to be strong functions of T^*, but depend only weakly on τ_m. The net effect is that the attenuated pulse seems to be essentially shifted in time by an amount grossly proportional to τ_m. However, if τ_m becomes too large ($\tau_m > 0.01$ s for $T^* = 1$, or $\tau_m > 0.1$ s for $T^* = 4$), the visual onset time τ_a vanishes. We shall see later that the character of the attenuated pulse changes when this happens, and that the small Dirac impulse occurring at $\tau = 0$ s is no longer negligible. In such cases, T_r becomes an ill-defined quantity. We shall first turn our attention to the cases where τ_m is a small quantity.

2.4 VARIATIONS OF THE PEAK AMPLITUDE

The peak amplitude A_p is most sensitive to the parameter T^*. The curves describing this dependence are shown in Fig. 7, where τ_M was kept constant ($\tau_M = 1000$ s) and A_p was plotted as a function of $1/T^*$ for several values of τ_m.

We see that if $\tau_m \ll 1$, A_p is essentially a linear function of $1/T^*$. This behaviour is consistent with the findings of previous investigators who used somewhat different attenua-

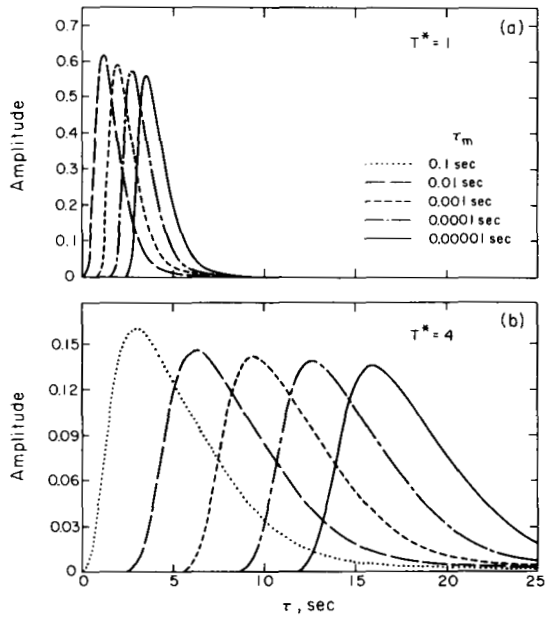

Figure 6. Effect of the short period cut-off τ_m of the absorption band on attenuated waveforms; $\tau_M = 1000$ s, $Q_m = 100$, (a) $T^* = 1$, (b) $T^* = 4$.

tion models. In particular, Azimi, Kalinin & Pivovarov (1968) showed that the peak amplitudes of attenuated, but undispersed (i.e. acausal) pulses do vary linearly with $1/t_u$ at constant Q, and that introduction of the dispersion required by the Kramers–Krönig relations does not change this behaviour significantly. The slopes of the curves on Fig. 7 are rather insensitive to τ_m, as could have been deduced from Fig. 6, except when τ_m becomes rather large. Some departure from linearity may be detected then, but this is precisely the case when τ_a vanishes and the pulse character changes. For $\tau_m = 0.1$ s. This phenomenon occurs for $T^* \simeq 2$. For smaller values of T^*, the pulse parameters will be discussed later.

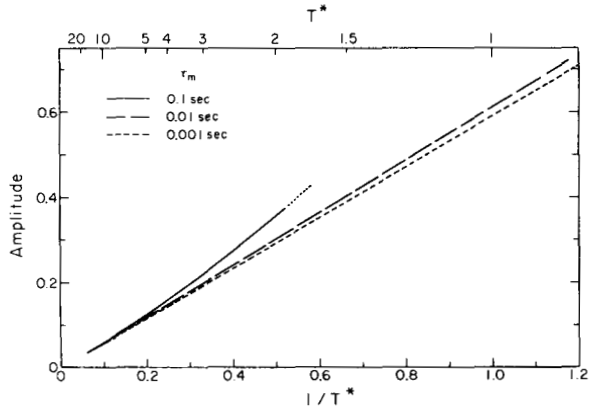

Figure 7. Variation of the peak amplitude of the attenuated pulse as a function of $1/T^*$, for selected values of τ_m; $\tau_M = 1000$ s.

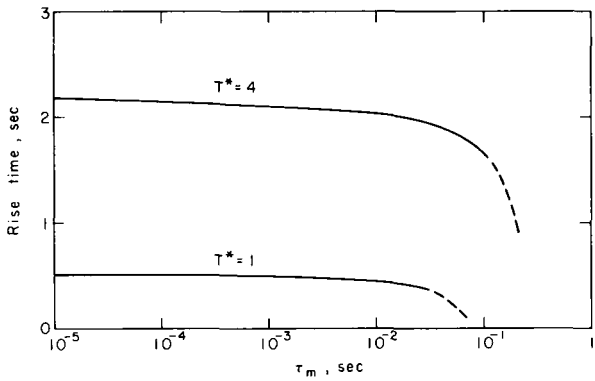

Figure 8. Variation of the rise time with τ_m for $T^* = 1$ and $T^* = 4$.

2.5 VARIATIONS OF THE RISE TIME

The dependence of T_r on τ_m, in the range where T_r may be defined as on Fig. 3, is shown on Fig. 8. Again $\tau_M = 1000$ s and two curves have been computed for $T^* = 1$ and $T^* = 4$ respectively. T_r is essentially independent of τ_m for small values of this parameter, but the rise time decreases abruptly – and actually vanishes – when τ_m reaches a critical value which depends on T^*.

The variation of T_r with T^* is shown on Fig. 9 for three values of τ_m. We see that T_r is a quasi-linear function of T^*, and that a small departure from linearity appears for rather large values of T^*. Again, for $\tau_m = 0.1$ s and $T^* \lesssim 2$, T_r becomes an ill-defined parameter and the curve loses its meaning.

The slopes of the curves shown on Fig. 9 are of interest: Stacey *et al.* (1975) argued, on the basis of observations made by Gladwin & Stacey (1974) that the rise times of attenuated pulses should be of the form

$$T_r = T_r^{(0)} + C\int_0^t Q^{-1}\,dt. \tag{2.4}$$

$T_r^{(0)}$ is a constant associated to the rise time of the initial pulse, and $C = 0.5$. The travel times of the attenuated pulses described by Stacey *et al.* (1975) were measured in microseconds,

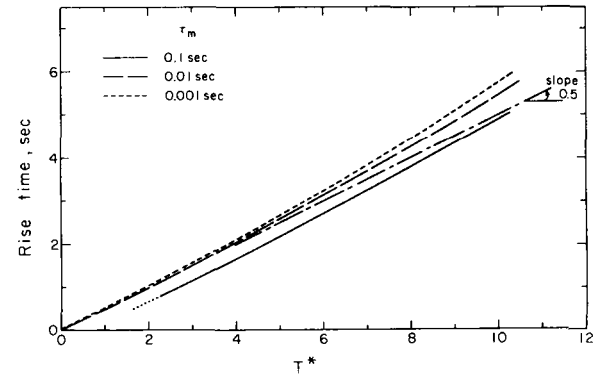

Figure 9. Variation of the rise time with T^* for selected values of τ_m. Also indicated is a reference line with slope 0.5.

and the medium was described as hard rock. This means that for any likely value of Q_m, the parameter T^* was very small for these experiments. Stacey *et al.* (1975) propose that (2.4), with $C = 0.5$ be considered a criterion that the attenuation operator must satisfy in order to be acceptable for geophysical purposes. We see that for $T^* < 4$ the relation $T_r = 0.5T^*$ fits the curves shown on Fig. 9 exceedingly well if τ_m is not too large. Actually, the data of Gladwin & Stacey imply $C = 0.53 \pm 0.04$. Even though the difference does not appear to be significant, it is gratifying to note that the calculations leading to Fig. 9 imply a value of C slightly greater than 0.5, particularly for larger values of T^*.

One interesting observation concerning the rise time T_r is illustrated on Fig. 10, where T_r is plotted against the 'relaxed' arrival time τ_R. This parameter is defined by

$$\tau_R = \frac{x}{V_R} - \frac{x}{V_u} = t_u \left[\sqrt{\frac{M_u}{M_R}} - 1\right]. \tag{2.5}$$

The surprising feature of Fig. 10 is that T_r is a linear function of τ_R. This is a rather remarkable result considering the great complexity of the expressions for $u(t, x)$ and $v(t, x)$ derived in Paper I. Again the result only holds as long as τ_m is not too large. This observation allows us to derive a semi-theoretical expression for T_r:

$$T_r = \alpha t_u \left[\sqrt{\frac{M_u}{M_R}} - 1\right], \tag{2.6}$$

where the coefficient α is a constant to be determined. In the limit of low-loss media, this expression may be written as

$$T_r \simeq \alpha \frac{2}{\pi} \frac{t_u}{Q_m} \ln \frac{\tau_M}{\tau_m}. \tag{2.7}$$

But we know from Fig. 9 that $T_r = 0.5T^*$ in the limit of small T^*, or large Q_m, that is, in the limit of small attenuation. Combination of these two observations leads to the expression

$$T_r = \frac{\pi t_u}{2 \ln \frac{\tau_M}{\tau_m}} \left[\frac{1}{\sqrt{1 - \frac{2}{\pi Q_m} \ln \frac{\tau_M}{\tau_m}}} - 1\right]. \tag{2.8}$$

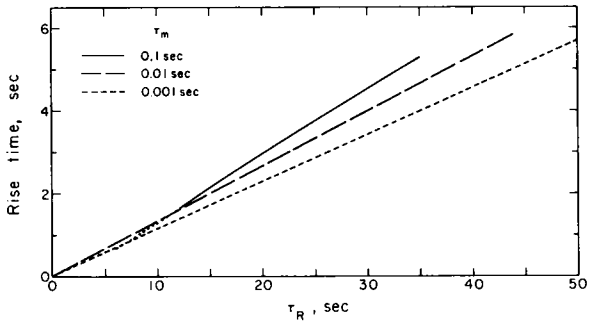

Figure 10. Variation of the rise time as a function of $\tau_R = (x/V_R) - (x/V_u)$, for selected values of τ_m.

It is clear that for small attenuation, T_r is very weakly dependent on τ_M and τ_m, in agreement with the results of Figs 5 and 8, and Taylor expansion of the bracket leads to the approximation $T_r = 0.5T^*$. It can be verified that (2.8) constitutes a very good fit to the curves shown on Fig. 9, again subject to the proviso that T_r be a well defined quantity.

2.6 VARIATIONS OF THE ARRIVAL TIME AND PEAK TIME

The pulse parameters τ_a and τ_p are shown on Fig. 11 as functions of τ_m for $T^* = 1$ and $T^* = 4$ respectively. It is clear that if the absorption band, as defined on Fig. 1, is extended to fairly high frequencies, the attenuated pulse is considerably delayed. The delay varies almost linearly with $\ln \tau_m$, and again there is an abrupt change in the character of the attenuated wave as τ_m increases past a critical value which, in turn, depends on T^*. The curves for τ_a and τ_p are almost parallel for a given value of T^*, which merely restates the result depicted on Fig. 8, namely, that the rise time T_r is nearly independent of τ_m if τ_m is small enough. In fact, there is an interesting observation concerning our choices for defining τ_a and T_r. To a very good precision, and if τ_m is small enough, we have the relation

$$\tau_p - \tau_a = 2T_r. \tag{2.9}$$

This result is only weakly dependent on our definition of τ_a. Indeed if the visual onset is defined on the basis of a detection threshold of 40 db below the peak amplitude instead of 60 db – that is, an amplitude ratio of 100 instead of 1000 – then the estimated values of τ_a are hardly modified. If a threshold level of -20 db is chosen, then τ_a will be increased by less than one second for $T^* = 4$, as a quick examination of Fig. 6 shows. We shall therefore adopt (2.9) as a convenient rule of thumb.

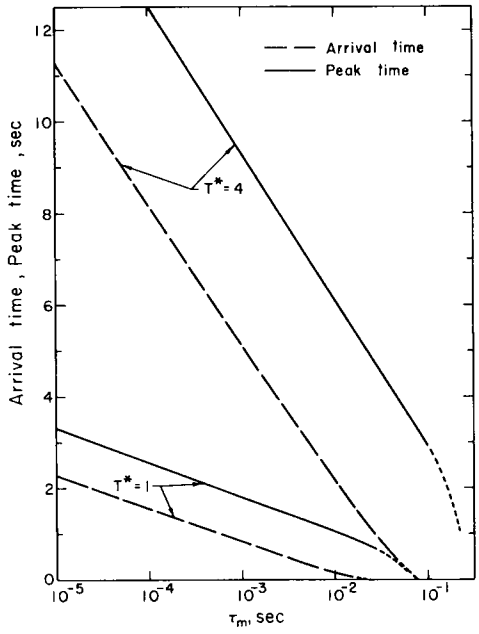

Figure 11. Arrival time and peak time as functions of τ_m for $T^* = 1$ and $T^* = 4$. τ_M is fixed at 1000 s, t_u at 500 s.

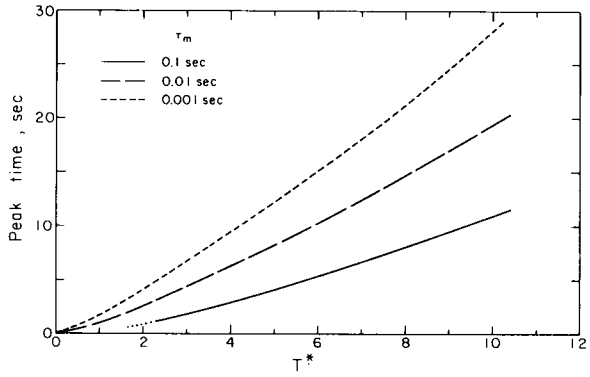

Figure 12. Peak time as a function of T^* for selected values of τ_m. τ_M = 1000 s, t_u = 500 s.

The variations of τ_p and τ_a with T^* are shown on Figs 12 and 13 respectively, for several values of τ_m. It is clear that there is a dramatic delay of the attenuated pulse with respect to the theoretical 'unrelaxed' arrival time as T^* increases, and that this effect increases sharply as τ_m becomes much smaller than one second. This is strongly reminiscent of the 'pedestal' effect advocated by Strick (1970) on the basis of his PL (power law) attenuation model. Strick considered a material with $Q = 40$ for $f = 100$ Hz, and a pulse with $t_u = 3.83$ s, so that T^* is of the order of 0.1; he then observed a 'pedestal' τ_a of about 0.6 s. This point is plotted on Fig. 13, and lies well above any of our own curves. A simple explanation of this discrepancy is that Strick's PL Model is precisely designed to model a medium with $Q(f)$ essentially constant to extremely high frequencies. In other words, the effective value of τ_m we should choose in order to compare our results with those of Strick must be exceedingly small. Thus our results are in fact quite consistent with Strick's (1970) 'pedestal' effect. This points to the need for the additional parameter τ_m, which is essentially absent from *ad hoc* attenuation models such as Futterman's (1962); Azimi *et al.* (1968), or Strick's (1970).

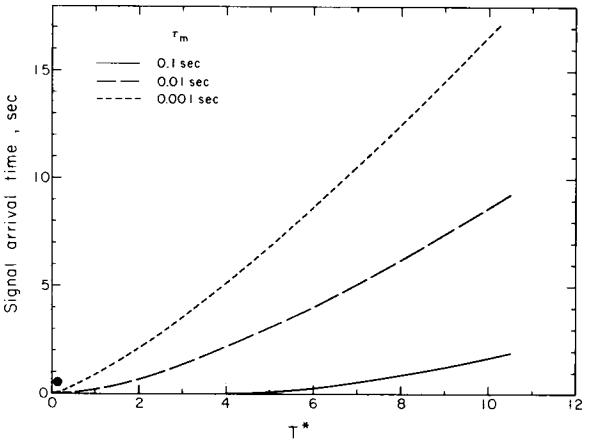

Figure 13. Arrival time as a function of T^* for selected values of τ_m. τ_M = 1000 s, t_u = 500 s. The point near the origin corresponds to Strick's (1970) result.

2.7 PULSE BEHAVIOUR FOR LARGE τ_m

In the course of the various parametric studies described above, we have observed time and again that the character of the attenuated pulse changes rather suddenly if τ_m becomes large enough or T^* small enough. In order to investigate this phenomenon in greater detail, we recall the results of Paper I concerning the precursor to the signal. On intuitive grounds only, it is clear that this precursor will become quite short for short propagation times t_u. In addition, if we go back to Fig. 1, it is clear that the high frequency asymptote of $\alpha(\omega)$ will take on smaller values if τ_m is increased at constant Q_m.

The precursor to the transient response is given by (e.g. Paper I)

$$u(\tau,x) \simeq \exp\left[-\frac{t_u}{\pi Q_m}(\tau_m^{-1}-\tau_M^{-1})\right] I_0\left(\sqrt{\frac{2}{\pi}\frac{t_u}{Q_m}\tau(\tau_m^{-2}-\tau_M^{-2})}\right), \tag{2.10}$$

where I_0 is the modified Bessel function of order zero, and the approximation is valid for $\tau \ll T^*/2\pi$. Time differentiation of this expression yields the precursor to the impulse response $v(t, x)$:

$$v(\tau,x) \simeq \sqrt{\frac{T^*}{2\pi}(\tau_m^{-2}-\tau_M^{-2})}\exp\left[-\frac{T^*}{\pi}(\tau_m^{-1}-\tau_M^{-1})\right]\tau^{-1/2} I_1\left(\sqrt{\frac{2T^*}{\pi}(\tau_m^{-2}-\tau_M^{-2})}\right). \tag{2.11}$$

The series expansion of $v(\tau, x)$ may be written in the form (e.g. Paper I)

$$v(\tau,x) \simeq \exp\left[-\frac{T^*}{\pi}(\tau_m^{-1}-\tau_M^{-1})\right]\left[\delta(\tau)+\frac{T^*}{2\pi}(\tau_m^{-2}-\tau_M^{-2})+0(\tau)\right]. \tag{2.12}$$

Let us assume that τ_m^{-1} is negligible, then the amplitude of the Dirac distribution at $\tau = 0$ is of the order of $\exp(-T^*/\pi\tau_m)$. It is, of course, negligible if T^* is large or τ_m small. For the sake of argument, assume that $T^* = \pi$, then this term is negligible unless τ_m is of the order of one second or longer. This explains why most of the curves described earlier suffer a rapid change as τ_m increases past a critical value. It is noteworthy that, as τ_m becomes quite large, or T^* very small, the exponential tends to unity and one finds the input Dirac pulse, which has not suffered any significant attenuation, as could have been predicted on an intuitive basis.

It is clear that the definitions of τ_a and T_r which we have adopted so far in this study become inappropriate if τ_m becomes too large. In fact, as soon as the terms shown in (2.11) become significant, one can argue that τ_a and T_r vanish for all practical purposes. Of course, this does not happen for any definite value of T^*/τ_m, but since this parameter appears in the exponent in (2.11), the transition will occur over a very small range of τ_m, at constant T^* of order unity.

In order to illustrate the behaviour of our solution near the critical value of τ_m, we note that the asymptotic expression for $v(t, x)$ which was used in the previous calculation is an intermediate time approximation. Those two asymptotic expressions should be matched to yield a qualitative waveform. This is done on Fig. 14, where $\tau_M = 1000$ s, $T^* = 4$ and τ_m takes the values 0.1, 0.3 and 1 s. Matching of the two asymptotic approximations was performed by connecting smoothly the two curves by hand in each case. The Dirac distribution at $\tau = 0$ is shown for the cases $\tau_m = 0.3$ and $\tau_m = 1$ s. We make no claim that the resulting pulse shapes are quantitatively accurate but we feel that the procedure yields a qualitative image of how these pulses get distorted as τ_m becomes large. Of course, if τ_m is

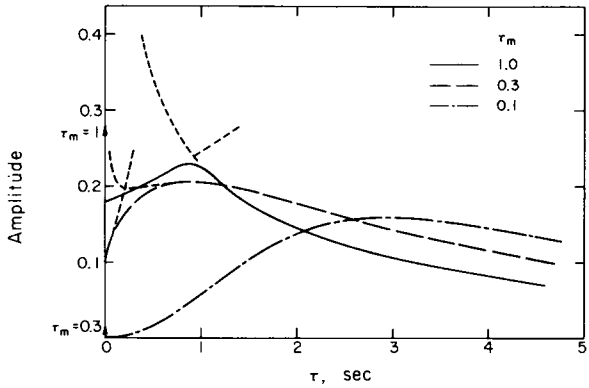

Figure 14. Evolution of the attenuated pulse for increasing τ_m. $T^* = 4$, $t_u = 500$ s, $\tau_M = 1000$ s. The curve for $\tau_m = 0.1$ s is the same as on Fig. 6(b). For $\tau_m = 0.3$ s and $\tau_m = 1$ s; the delta function occurring at $\tau = 0$ is represented by a vertical arrow in each case. The waveforms are drawn by smoothly connecting two asymptotic forms, for τ very small and τ moderately large respectively.

increased to values much greater than unity in this case, the pulse shape reduces to a very sharp spike at $\tau \simeq 0$ followed by an exponentially decaying 'tail'.

When convolved with a wavelet, or a source function, and an instrument response, the pulses depicted on Fig. 14 will of course distort the attenuated wave shape. However, no delay in the visual arrival time due to attenuation is expected in that case. Note also that, since the absorption band does not extend to very high frequencies any more, a Fourier transform procedure using (1.4) as the 'Q operator' will yield acceptable results in that case for all practical purposes, as shown by Butler (1978, in preparation). On the contrary, it was shown in Paper I that such a procedure will yield the correct wave shape if $\tau_m \ll 1$ but not the correct onset time nor the correct peak time, unless a very large number of points is used in the FFT calculation.

3 Implications for seismology

The attenuation of seismic waves has long been an object of considerable interest to seismologists. Abundant literature exists on the subject and it is not our purpose to review it. Such a review may be found in Stacey *et al.* (1975). We shall confine our discussion to the implications of the specific attenuation model used in Paper I and this paper.

The implications of the attenuation model used here for both short-period (body waves) seismology and long-period (free oscillations) seismology have been recently at the focus of several investigations. Liu *et al.* (1976) formulated the problem in detail, and compared the present model with previously proposed models for the attenuation operator. Anderson *et al.* (1977) argued that the attenuation of seismic waves was associated with the coincidence of a broad absorption band with the seismic frequency range. Anderson & Hart (1977) reviewed the available data and favoured a physical attenuation mechanism based on a grain boundary relaxation model. In this fashion, they explained the higher attenuation of shear waves, the weak frequency dependence of average Q values, and the variation of Q with depth. Kanamori & Anderson (1977) reviewed the effects of dispersion associated with attenuation on surface wave dispersion curves and free oscillation periods.

The present investigation is of a somewhat different nature in the sense that we do not consider quasi-harmonic vibrations of the medium, but rather transient signals having a rather broad frequency spectrum but a limited duration in the time domain. The main

question which arises then may be formulated as follows: what rheological parameter of the Earth is measured by body wave travel times? Jeffreys & Crampin (1970) and Jeffreys (e.g. Jeffreys 1975) have investigated this question using a modified version of rheological law of Lomnitz (1957), in which the absorption band extends to very high frequencies, and concluded that attenuation plays an important role in the interpretation of travel time data.

The first conclusion that the preceding section leads us to is that the apparent wave velocity deduced from the travel times of short pulses is not related in any straightforward way to either V_u or V_R, nor is it related to the phase velocity at any given frequency. Moreover, since τ_a is not quite a linear function of T^*, the mean propagation velocity measured by the pulse travel time will actually decrease slightly with increasing distance. Further, since T^* will be smaller for P waves than for S waves, Poisson's ratio will be slightly overestimated, with respect to its 'elastic' (high-frequency) theoretical value. It is clear from the parametric study performed above that the magnitude of such biases will depend on the high frequency cut-off value τ_m^{-1}.

3.1 TRAVEL TIMES OF MANTLE S WAVES

In order to obtain a crude estimate of what the value of τ_m might be in the Earth's mantle, we shall assume:

(1) that τ_m is independent of radius in the Earth;

(2) that at any radius, there is only one absorption band which includes a fiducial period which we choose to be 1000 s.

As shown by Liu *et al.* (1976), as well as elsewhere in the literature quoted here, one may in principle compute a 'one second' earth model, in which the radial variations of the wave velocities actually represent the radial variation of the phase velocities at one hertz. This may be done if the complete absorption band is known at each radius. In practice (e.g. Anderson & Hart 1977; Hart 1977) it is usually assumed that $1 < f_M$, that is, the seismic absorption band extends – with constant $Q^{-1}(f)$ – to frequencies higher than one hertz; this is also equivalent to $\tau_m < 1/2\pi$. In such a case, for any frequency $f_m < f < f_M$, we have the classical dispersion relation (e.g. Liu *et al.* 1976)

$$\frac{V_p(f)}{V_p(1)} \simeq 1 + \frac{1}{\pi Q_m} \ln f. \tag{3.1}$$

When this relation is applied to long-period seismic data – in particular, free oscillation periods – and when a model is chosen for $Q_m(r)$, then a 'one second' earth model may be derived, and the body wave travel time curves may be computed for this model. Let $t_1(\Delta)$ be such a travel time curve, and let $t_u(\Delta)$ be the unknown travel time curve for an 'unrelaxed' earth model. Then

$$t_1(\Delta) = t_u(\Delta) + \tau_1'(\Delta). \tag{3.2}$$

The correction term $\tau_1'(\Delta)$ may be computed easily under the following assumptions:

(1) that the dispersion curve – Fig. 1(b) – applicable in that case is that corresponding to the average Q for this particular ray;

(2) that a single value of τ_m applies to the whole mantle.

Let $V'_p(1)$ be the average wave velocity along the particular ray under consideration, then for $f_m < 0.001 < 1 < f_M$ we have from (3.1)

$$\frac{V'(1)}{V_u} = \left(1 + \frac{2.2}{Q_m}\right)\frac{V(0.001)}{V_u}, \tag{3.3}$$

$$\tau'_1(\Delta, \tau_m) = t_u\left[\frac{V_u}{V'(1)} - 1\right], \tag{3.4}$$

where V_u is the average unrelaxed velocity, $V(0.001)$ the average of the phase velocity at 0.001 Hz, and Q_m the average Q along the ray. (3.3) and (3.4) permit the theoretical calculation of the correction term τ'_1 given an earth model, a Q model and a choice of τ_m · $\tau'_1(\Delta, \tau_m)$ will be negative for large τ_m and positive for small τ_m.

If we now turn to the observed travel times $t_a(\Delta)$, the equivalent of (3.2) is

$$t_a(\Delta) = t_u(\Delta) + \tau_a(T^*, \tau_m), \tag{3.5}$$

where τ_a may be calculated as in Figs 11, 12, 13 and T^* may be computed from the model for each ray. Elimination of the unknown $t_u(\Delta)$ between (3.2) and (3.5) yields

$$t_1(\Delta) - t_a(\Delta) = \tau'_1(\Delta, \tau_m) - \tau_a(T^*, \tau_m), \tag{3.6}$$

where the only free parameter is now τ_m.

We applied this procedure to Hart's (1977) model QM3, which is a 'one second' earth model, and where the radial variation of Q is given by Anderson & Hart's (1977) SL1 model. The phases we considered were mantle P and S waves with a surface focus, and the relevant parameters are listed in Tables 1 and 2 respectively. In order to evaluate the left-hand side of (3.6), a specific data set had to be chosen in each case. We adopted the tables of Herrin

Table 1. Mantle P waves travel time residuals for model QM3.

Δ degrees	Travel time QM3 (s)	Average Q	T^*	1968 tables (s)	QM3 residual (s)
30	369.4	486	0.76	369.5	−0.1
40	455.6	518	0.88	455.7	−0.1
50	534.8	575	0.93	535.2	−0.4
60	606.8	660	0.92	607.4	−0.6
70	672.2	791	0.85	672.7	−0.5
80	730.3	936	0.78	730.6	−0.3
90	781.0	898	0.87	780.7	+0.3

Table 2. Mantle S waves travel time residuals for model QM3.

Δ degrees	Travel time QM3 (s)	Average Q	T^*	JB tables (s)	QM3 residual (s)
30	668.4	194	3.45	670.2	−1.8
40	819.4	207	3.96	824.5	−5.1
50	966.9	226	4.27	968.6	−1.7
60	1100.5	256	4.30	1102.6	−2.1
70	1222.5	294	4.16	1225.6	−3.1
80	1334.4	359	3.72	1336.5	−2.1
90	1431.9	400	3.58	1434.5	−2.6

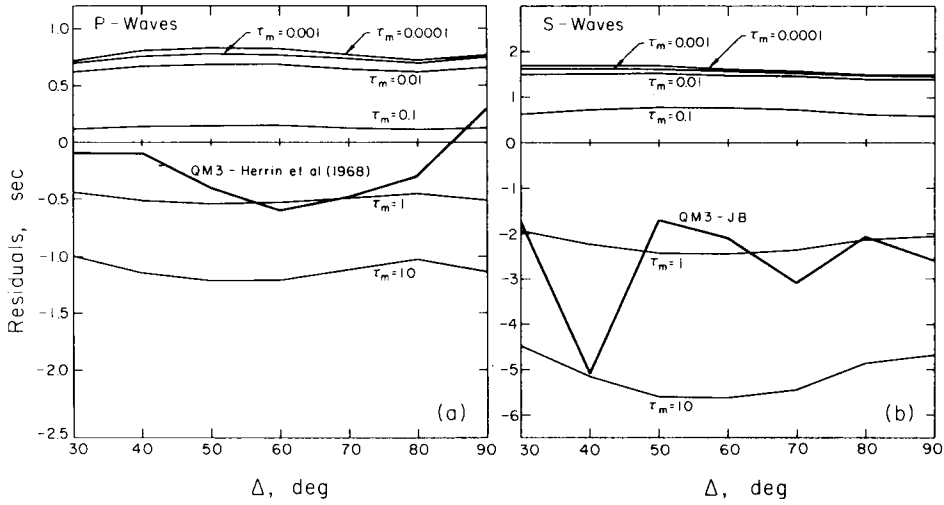

Figure 15. Travel-time residuals of a 'one second' earth model. (a) *P* waves, (b) *S* waves, as a function of Δ. QM3 is a 'one second' earth model obtained under the assumption that $\tau_m \ll 1$. The curves τ_m = constant (τ_m in seconds), are what the theoretical residuals should be if τ_m were in fact finite in the mantle, and independent of radius. The various assumptions used here are described in the text.

(1968) for *P* waves and the JB Tables for *S* waves. The right-hand side of (3.6) was evaluated for several values of τ_m and comparison with the results of Tables 1 and 2 is provided on Fig. 15(a) and (b). It appears that, *under the restrictive assumptions enunciated above,* τ_m should be of the order of one second in the Earth's mantle. This conclusion depends further on the following additional assumptions:

(1) that the attenuation in the mantle may be modelled by a spectrum of relaxation mechanisms such as the one we use here;

(2) that model SL1 is a valid representation of the radial variation of Q_m;

(3) that the data leading to the derivation of model QM3 all have frequencies lying within the same absorption band, and

(4) that the tables chosen to represent $t_a(\Delta)$ do not suffer from a systematic bias.

With regard to *P* waves, Fig. 15(a) is actually not very conclusive since the difference between the curves for $\tau_m = 0.1$ and $\tau_m = 1$ is only of the order of 0.5 s, less than the uncertainties in the travel times. However, one must point out that the JB tables are grossly 2.5–3 s late compared to the 1968 tables, and that recent travel time studies are also late with respect to the 1968 tables, by up to 2 s (e.g. Cleary & Hales 1966; Carder, Gordon & Jordan 1966; Hales, Cleary & Roberts 1968). Thus the adoption of any of these data sets for $t_a(\Delta)$ would shift the QM3 curve downward on Fig. 15(a), and imply even larger values of τ_m.

With regard to *S* waves, the observations of Helmberger & Engen (1974), those of Hart (1975); Hales & Roberts (1970); Ibrahim & Nuttli (1967), as well as travel times computed from models such as those of Jordan & Anderson (1974); Anderson & Hart (1976), are all late with respect to JB. This may be explained, at least in some cases, on the basis of regional variations. The key point here is that, should we change the base line on Fig. 15(b) from JB to any one of these data sets, the QM3 curve would also be shifted downwards, implying larger values of τ_m. Jeffreys (1970) reports some observations by Arnold with negative JB residuals; similarly Sengupta (1975) finds JB residuals of the order of – 2 s. However, these

latter studies involve deep focus events and are not directly applicable to Fig. 15 since different T^* values would have to be used.

Note that the sharp structure in the QM3 curve on Fig. 15(b) near $\Delta = 40^\circ$ would disappear if, for instance, the data of Ibrahim & Nuttli (1967) were used as reference.

In opposition to the foregoing arguments, it is clear that our definition of τ_a (see Fig. 3) may very well lead to a bias. It is highly improbable that observations actually involve the -60 db definition of Fig. 3, especially if noise is present. If a 20 db threshold is adopted, then the curves representing the various values of τ_m on Fig. 15(b) might be shifted downwards, by an amount of the order of a second or less, and τ_m could be somewhat smaller. (This effect would be quite small when P waves are concerned.)

Another possible effect is that QM3 may be over-corrected. This would be the case if the Q values for free oscillations are underestimated, which is a real possibility in view of the well known difficulties in estimating these values. But increasing Q would affect both t, (Δ) and $\tau_1'(\Delta)$ by comparable amounts in (3.6), so that one may expect the effect on the estimation of τ_m to be rather small.

It is noteworthy that if observable travel times should be about one second earlier than the 1968 tables for P waves and about four seconds earlier than JB for S waves, or if QM3 should be in fact too fast by the same amounts, then no conclusion could be reached as to the value of τ_m since (3.6) becomes very insensitive to τ_m when τ_m becomes small.

Considering the large number of uncertainties involved here, the actual estimate of τ_m cannot be very reliable. If τ_m were as large as 1 s, a number of important and rather disquieting, but hopefully testable consequences would follow. The first is that $Q(f)$ must increase as a function of frequency for periods less than about 50 s. It must be emphasized that this does not mean that body waves with an apparent period of a few seconds would not be strongly attenuated. As may be seen on Fig. 1, the attenuation coefficient $\alpha(f)$ at high frequencies depends both on the width of the absorption band and on the value of Q_m. Thus $\alpha(1)$, for instance, depends strongly on the frequency dependence of Q for periods longer than 60 s if we adopt this particular model. The difficulty is that there is at present no convincing evidence that Q^{-1} should decrease as $1/f$ for periods shorter than 50 s. In fact, a constant Q model explains the relative attenuation rates of sP and sS phases from the Borrego Mountain earthquake in a period range from 0.5 to 15 s (Burdick 1977). Since this study involves computation of synthetic seismograms using the attenuation operator of Futterman (1962), one may deduce from Figs 6b and 14 that τ_m should not be any larger than 0.1 s, in contradiction with the implications of Fig. 15. Preliminary work by Butler (1978, in preparation), using the present model and taking into account instrumental responses, indicates that the data of Burdick (1977) do not allow values of τ_m greater than 0.25 s. The corresponding curve on Fig. 15(b) would lie about 0.5 s below the JB base line, and about 2 s above QM3.

In the absence of more convincing evidence, we do not feel that a value of $\tau_m = 0.25$ s is irreconcilable with Fig. 15.

Although some frequency dependence of Q has been reported (e.g. Sato & Espinosa 1967; Yoshida & Tsujiura 1975), it is not clear at this point whether observations can be explained with such a large value of τ_m, nor whether these observations require rejecting such a model. If τ_m is large enough, then the rise time of observations, once corrected for instrumental effects, should be a good measure of the rise time at the source. This should hold particularly for P waves since $T^* \simeq 1$ in that case. One instructive experiment would be to compare the rise time of P waves from explosive sources at teleseismic distances on a very short-period (< 0.1 s) instrument with the same rise time measured at very short distances. In addition, we note that on Fig. 14 the peak amplitude, which is insensitive to τ_m for

$\tau_m < 0.1$ s, doubles as τ_m rises from 0.1 to 1 s. However, the total area under the curve is not affected so that moment estimates from teleseismic body waves are not affected.

Another interesting consequence of our model is that body wave travel times should measure the unrelaxed properties of the mantle. For relevant values of T^* it is clear from the results of the previous section that τ_a vanishes or is very small in that case.

Finally, one should point out that the present discussion does not preclude alternate explanations for the travel time 'baseline' discrepancy between body wave observations and free oscillation models. In particular, the possibility of a regional bias, which is often favoured in the literature is not incompatible with the present results.

3.2 OBSERVATIONS OF MULTIPLE *ScS* WAVES

From observations of multiple *ScS* phases Jordan & Sipkin (1977) and Sipkin & Jordan (1976) estimated the two-way travel time of *ScS* at vertical incidence to be 937.3 s, and the average Q to be 156 or $T^* = 6$. This means that the values of T^* for ScS_2, ScS_3, ScS_4 should be 12, 18 and 24 respectively. Had they measured differential times of the type ScS_n–ScS_{n-1} by estimating the arrival times of these phases, then because of the upward curvature of τ_a as a function of T^* (e.g. Fig. 12), their estimate of the two-way travel time from ScS_4–ScS_3 should be somewhat longer than that from ScS_2–ScS. The effect may be calculated to be of the order of one or two seconds. However, such differential travel times are usually estimated by cross-correlating the two phases (e.g. Sipkin & Jordan 1975; Okal & Anderson 1975). In that case, the relevant quantity is τ_p. We have seen that, for small τ_m, $\tau_p - \tau_a \simeq 2T_r$, and that the rise time T_r increases rather rapidly with T^*, also with an upward curvature (Fig. 9). Thus two effects may be expected from our model: (1) the two-way *ScS* travel time as estimated from ScS_n–ScS_{n-1} should increase slightly with increasing n, and more importantly, (2) the cross-correlation method should lead to overestimates of the differential time. This last bias may be quite large and reach five seconds or more (Fig. 9) if τ_m is small and we compare waves with such large T^* values. For normal oceanic regions, Sipkin & Jordan (1976) published the following estimates of the JB two-way residuals of *ScS*:

	Mean residual	Standard error in the mean
From ScS_2–ScS	3.4	±0.50
From ScS_3–ScS_2	4.1	±0.55
From ScS_4–ScS_3	5.4	±0.58

Although these observations exhibit a trend analogous to our prediction, the data are unfortunately too scanty to permit a positive conclusion (Jordan 1977, private communication). On the other hand, the mean two-way *ScS* travel time obtained from their complete data set is 937.3 s; the Jeffreys–Bullen time is 935.7 s and model QM3 predicts 931.8 s. QM3 has a JB residual of −2.9 s, in agreement with Fig. 15 and $\tau_m = 1$. Sipkin & Jordan's estimate is only 1.6 s greater than the JB time. The lack of a large bias also points to a rather large value of τ_m, and so does the fact that ScS_3 or ScS_4 do not exhibit apparent periods much larger than *ScS* in the data presented by Sipkin & Jordan (1976). This argument is, of course, a rather crude one and a more refined analysis, involving computation of synthetic seismograms is currently underway (Butler 1977).

The arguments presented in this section depend critically on the various assumptions made at the beginning, and one may legitimately question several of these hypotheses. It is

conceivable that the 'one-second' earth model QM3 may have to be revised as better data become available, and that this difficulty should disappear. Another source of uncertainty lies in the actual attenuation mechanism which we used in this paper. There is no reason why the relaxation spectrum should possess a sharp high-frequency cut-off τ_m, or that τ_m should be independent of position in the mantle. In fact, Anderson (1976) proposed a physical model of attenuation based on a grain boundary relaxation mechanism; the absorption band associated with this mechanism is controlled by thermodynamical conditions which are outlined by Anderson & Hart (1977). Anderson (1976) suggests that τ_m, τ_M, and Q_m are all strongly dependent on depth in the Earth's mantle. It is clear that the implications of such behaviour of the attenuation band must be analysed carefully before the present argument is purused any further.

Additional relaxation mechanisms with characteristic periods shorter than τ_m could be added to the spectrum, in such a way that Q^{-1} would not decay as fast as ω^{-1} at high frequency. $\alpha(\omega)$ would then continue to increase as a function of frequency instead of reaching a plateau, and the waveforms on Fig. 15 would have to be changed somewhat. In addition, if there are additional absorption bands at frequencies higher than the seismic band, the Dirac distributions on Fig. 15 will be attenuated and dispersed accordingly. In that case the unrelaxed velocity V_u would have no bearing on seismic observations any more. Furthermore, the effect of layers in the Earth where τ_m might be very small, such as the near surface layers, is rather difficult to assess using the present elementary theory. Finally, the plane wave attenuation characteristics used here do not take into account the results of Borcherdt (1973a, b, 1977), who showed that homogeneous plane waves rapidly become inhomogeneous when they propagate through a layered attenuating medium. Such complications lie outside the scope of the present discussion.

However, given the proposed attenuation mechanism, as well as this particular attenuating earth model, one is led to the conclusion that there exists a frequency window in the vicinity of 1 Hz in which the density or efficiency of relaxation mechanisms is lower than at longer periods, and that the quality factor is not independent of frequency in that range.

Conclusion

We have investigated the consequences of the linear relaxation model of attenuation on the propagation of one-dimensional pulses. This model, which can easily yield a frequency independent quality factor over the seismic frequency band satisfies the constraints proposed by Stacey *et al.* (1975). It is also consistent with the grain boundary relaxation model of Anderson & Hart (1977) which satisfies a broad range of seismic observations.

The important parameters controlling the propagation of attenuated pulses are $T^* = t_u/Q_m$, as well as the high-frequency cut-off of the relaxation spectrum τ_m. This last parameter is the major new degree of freedom provided by this model with respect to formerly proposed attenuation models. The visual arrival time of the pulse, the peak time, and the rise time were shown to depend rather strongly on T^* and τ_m provided that $\tau_m \ll 1$. However, comparison of body wave seismic observations – more particularly, body wave travel times in the Earth's mantle – with an earth model derived from long-period seismic data leads to the conclusion that τ_m is rather large in the Earth's mantle, possibly of the order of one second.

In spite of the oversimplified nature of the model, and of the many approximations and assumptions made, we hypothesize that there may be a gap in the seismic absorption band in the vicinity of one hertz, and body wave observations tend to support the idea that such a gap would have to lie rather towards higher frequencies. Additional studies involving calcula-

tions of synthetic seismograms both from normal mode theory for longer periods and from body wave theory for higher frequencies are required in order to reconcile all the evidence available. In particular, one must include the possibility of a strong variation of τ_m with depth in the Earth, which will require significant extension of the present analysis.

Acknowledgments

Lively and instructive discussions with R. Hart, L. Burdick, G. Mellman, and R. Butler are gratefully acknowledged. D. Anderson and H. Kanamori as well as numerous colleagues offered helpful criticism. V. Cormier provided a useful review of the manuscript.

This research was supported by the Advanced Research Projects Agency of the Department of Defense and was monitored by the Air Force Office of Scientific Research under Contract No. AFOSR F49620-77-C-0022. Contribution No. 2914, Division of Geological and Planetary Sciences, California Institute of Technology, Pasadena, California 91125.

References

Anderson, D. L., 1976. Q of the Earth and its physical interpretation, *EOS Trans. Am. geophys. Un.*, **57** 958.

Anderson, D. L. & Hart, R. S., 1976. An earth model based on free oscillations and body waves, *J. geophys. Res.*, **81**, 1461–1475.

Anderson, D. L. & Hart, R. S., 1977. The Q of the Earth, *J. geophys. Res.*, in press.

Anderson, D. L., Kanamori, H., Hart, R. S. & Liu, H.-P., 1977. The Earth as a seismic absorption band, *Science*, **196**, 1104–1106.

Anderson, D. L. & Kovach, R. L., 1964. Attenuation in the mantle and rigidity of the core from multiple reflected core phases, *Proc. Nat. Acad. Sci.*, **51**, 168.

Azimi, Sh. A., Kalinin, A. V. & Pivovarov, B L., 1968. Impulse and transient characteristics of media with linear and quadratic absorption laws, *Izv. Earth Physics*, **2**, 42–54 (English Translation).

Borcherdt, R. D., 1973a. Energy and plane waves in linear viscoelastic media, *J. geophys. Res.*, **78**, 242, 2453.

Borcherdt, R. D., 1973b. Rayleigh-type surface wave on a linear viscoelastic half-space, *J. acoust. Am.*, **54**, 1651–1653.

Borcherdt, R. D., 1977. Reflection and refraction of type II S waves in elastic and anelastic media, *Bull. seism. Soc. Am.*, **67**, 43–68.

Brillouin, L., 1960. *Wave propagation and group velocity*, Academic Press, New York.

Burdick, L. J., 1977. Broad band studies of body waves, *PhD thesis*, California Institute of Technology.

Carder, D. S., Gordon, D. W. & Jordan, J. N., 1966. Analysis of surface foci travel times, *Bull. seism. Soc. Am.*, **56**, 815.

Carpenter, E. W., 1967. Teleseismic signals calculated for underground, underwater, and atmospheric explosions, *Geophys.*, **32**, 17–32.

Chu, B. T., 1962. Stress waves in isotropic linear viscoelastic materials, *J. de Mécanique*, **1**, 439–462.

Cleary, J. R. & Hales, A. L., 1966. An analysis of the travel times of P waves to North American stations in the distance range of 32° to 100°, *Bull. seism. Soc. Am.*, **56**, 467.

Elices, M. & García-Moliner, F., 1968. Wave packet propagation and frequency-dependent internal friction, in: *Physical acoustics*, ed. V, Mason, Academic Press, New York.

Futterman, W. I., 1962. Dispersive body waves, *J. geophys. Res.*, **67**, 5279–5291.

Geller, R. J. & Stein, S., 1977. Source mechanism and attenuation studies using split normal modes,

Gladwin, M. T. & Stacey, F. D., 1974. Anelastic degradation of acoustic pulses in rock, *Phys. Earth planet Int.*, **8**, 332.

Gurevich, G. I., 1964. A basic feature of the propagation and attenuation of seismic vibrations, in: *Aspects of the dynamic theory of seismic wave propagation collection*, vol. 7, Sbornik.

Hales, A. L., Cleary, J. R. & Roberts, J. L., 1968. Velocity distributions in the lower mantle, *Bull. seism. Soc. Am.*, **58**, 1975.

Hales, A. L. & Roberts, J. L., 1970. Shear velocities in the lower mantle and the radius of the core, *Bull. seism. Soc. Am.*, **60**, 1427.

Hart, R. S., 1975. Shear velocity in the lower mantle from explosion data, *J. geophys. Res.*, **80**, 4889.
Hart, R. S., 1977. The distribution of seismic velocities and attenuation in the Earth, *PhD thesis*, California Institute of Technology.
Helmberger, D. V. & Engen, G. R., 1974. Upper mantle shear structure, *J. geophys. Res.*, **79**, 4017.
Helmberger, D. V. & Wiggins, R. A., 1971. Upper mantle structure of middle-western United States, *J. geophys. Res.*, **76**, 3229.
Herrin, E. (Chairman), 1968. Seismological Tables for *P* phases, *Bull. seism. Soc. Am.*, **58**, 1193.
Ibrahim, A. K. & Nuttli, O., 1967. Travel time curves and upper mantle structure from long period *S* waves, *Bull. seism. Soc. Am.*, **57**, 1063.
Jeffreys, Sir Harold, 1970. *The Earth*, 5th edn, Cambridge University Press, London.
Jeffreys, Sir Harold, 1975. The importance of damping in geophysics, *Geophys. J. R. astr. Soc.*, **40**, 23.
Jeffreys, H. & Crampin, S., 1970. On the modified Lomnitz Law of damping, *Mon. Not. R. astr. Soc.*, **147**, 295.
Jordan, T. H. & Anderson, D. L., 1974. Earth structure from free oscillations and travel times, *Geophys. J. R. astr. Soc.*, **36**, 411.
Jordan, T. H. & Sipkin, S. A., 1977. Estimation of the attenuation operator for multiple *ScS* waves, *Geophys. Res. Lett.*, **4**, 167.
Kanamori, H. & Anderson, D. L., 1977. Importance of physical dispersion in surface wave and free oscillation problems: Review, *Rev. Geophys. Space Phys.*, **15**, 105–112.
Liu, H.-P., Anderson, D. L. & Kanamori, H., 1976. Velocity dispersion due to anelasticity; implications for seismology and mantle composition, *Geophys. J. R. astr. Soc.*, **47**, 41–58.
Lomnitz, C., 1957. Linear dissipation in solids, *J. appl. Phys.*, **28**, 201–205.
Minster, J. B., 1978. Transient and impulse responses of a one-dimensional linearly attenuating medium – I. Analytical results, *Geophys. J. R. astr. Soc.*, **52**, 479.
Okal, E. A. & Anderson, D. L., 1975. A study of lateral inhomogeneities in the upper mantle by multiple *ScS* travel time residuals, *Geophys. Res. Lett.*, **2**, 313.
Sato, R. & Espinosa, A. F., 1967. Dissipation in the Earth's mantle and rigidity and viscosity in the Earth's core determined from waves multiply reflected from the mantle core boundary, *Bull. seism. Soc. Am.*, **70**, 3935.
Sengupta, M., 1975. The structure of the Earth's mantle from body wave observations, *PhD thesis*, Massachusetts Institute of Technology.
Sipkin, S. A. & Jordan, T. H., 1975. Lateral heterogeneity of the upper mantle determined from the travel times of *ScS*, *J. geophys. Res.*, **80**, 1474.
Sipkin, S. A. & Jordan, T. H., 1976. Lateral heterogeneity of the upper mantle determined from the travel times of multiple *ScS*, *J. geophys. Res.*, **81**, 6307.
Stacey, F. D., Gladwin, M. T., McKavanagh, B., Linde, A T. & Haste, L. M., 1975. Anelastic damping of acoustic and seismic pulses, *Geophys. Surv.*, **2**, 133–151.
Strick, E., 1970. A predicted pedestal effect for pulse propagation in constant-*Q* solids, *Geophys.*, **35**, 387–403.
Yoshida, M. & Tsujiura, M., 1975. Spectrum and attenuation of multiply reflected core phases, *J. Phys. Earth*, **23**, 31.